



**SPECTROSCOPY AND ORBITAL ANALYSIS OF BRIGHT
BOLIDES OBSERVED OVER THE IBERIAN PENINSULA FROM
2010 TO 2012**

| | |
|-------------------------------|---|
| Journal: | <i>Monthly Notices of the Royal Astronomical Society</i> |
| Manuscript ID: | MN-13-1337-MJ.R2 |
| Manuscript type: | Main Journal |
| Date Submitted by the Author: | 05-Jul-2013 |
| Complete List of Authors: | Madiedo, José; Universidad de Huelva, Facultad de Ciencias Experimentales; Universidad de Sevilla, Departamento de Física Atómica, Molecular y Nuclear Trigo-Rodríguez, Josep; Institute of Space Sciences, Astrophysics; Institut d'Estudis Espacials de Catalunya, Ortiz, Jose; Instituto de Astrofísica de Andalucía, Solar System Castro-Tirado, Alberto; Instituto de Astrofísica de Andalucía (IAA-CSIC), Astrofísica Pastor, Sensi; Observatorio Astronómico de La Murta, de los Reyes, Jose; Observatorio Astronómico de La Murta, |
| Keywords: | meteors, meteoroids < Solar System |
| | |

SPECTROSCOPY AND ORBITAL ANALYSIS OF BRIGHT BOLIDES OBSERVED OVER THE IBERIAN PENINSULA FROM 2010 TO 2012

José M. Madiedo^{1,2}, Josep M. Trigo-Rodríguez³, José L. Ortiz⁴, Alberto J. Castro-Tirado⁴, Sensi Pastor⁵, José A. de los Reyes⁵ and Jesús Cabrera-Caño²

¹ Facultad de Ciencias Experimentales, Universidad de Huelva, 21071 Huelva, Spain.

² Departamento de Física Atómica, Molecular y Nuclear. Facultad de Física.
Universidad de Sevilla. 41012 Sevilla, Spain.

³ Institut de Ciències de l'Espai (CSIC-IEEC), Campus UAB, Facultat de Ciències,
Torre C5-parell-2^a, 08193 Bellaterra, Barcelona, Spain.

⁴ Instituto de Astrofísica de Andalucía, CSIC, Apt. 3004, 18080 Granada, Spain.

⁵ Observatorio Astronómico de La Murta. Molina de Segura, 30500 Murcia, Spain.

ABSTRACT

We present the analysis of the atmospheric trajectory and orbital data of four bright bolides observed over Spain, one of which is a potential meteorite dropping event. Their absolute magnitude ranges from -10 to -11. Two of these are of sporadic origin, although a Geminid and a κ -Cygnid fireball are also considered. These events were recorded in the framework of the continuous fireball monitoring and spectroscopy campaigns developed by the Spanish Meteor Network (SPMN) between 2010 and 2012. The tensile strength of the parent meteoroids is estimated and the abundances of the main rock-forming elements in these particles are calculated from the emission spectrum obtained for three of these events. This analysis revealed a chondritic nature for these meteoroids.

KEYWORDS: meteorites, meteors, meteoroids.

1 INTRODUCTION

1
2
3 The detailed study of bright fireballs is one of the aims of the Spanish Meteor Network
4 (SPMN), as these allow us to collect very valuable information on the origin and
5 properties of large meteoroids that, under appropriate conditions, can give rise to the
6 relatively rare meteorite-dropping events. Thus, one of the main goals of our meteor
7 network is the analysis of the physico-chemical properties of these meteoroids from
8 multiple station images. For this purpose we perform a systematic monitoring of the
9 night sky with the aim to obtain data to improve our knowledge of the mechanisms that
10 deliver these materials to the Earth. Nowadays we operate 25 meteor observing stations
11 that monitor the night sky over Spain and neighbouring regions, which is equivalent to
12 an area of more than 500.000 km². These stations provide useful information for the
13 determination of radiant, orbital and photometric parameters (Madiedo and Trigo-
14 Rodriguez 2008; Trigo-Rodriguez et al. 2007, 2009a; Madiedo et al. 2013a, 2013b,
15 2013c). Besides, we focus special attention on the study of the chemical composition of
16 meteoroids from the analysis of the emission spectrum produced when these particles
17 ablate in the atmosphere (Trigo-Rodriguez et al 2007, 2009a; Madiedo et al. 2013a,
18 2013b, 2013c). For this reason, a significant part of our effort has focused on the
19 deployment of spectrographs at some of our meteor observing stations. The first of
20 these devices, which were based on high-sensitivity CCD video cameras endowed with
21 attached holographic diffraction gratings, started operation in 2006 from our station in
22 Sevilla, but also from a mobile station operated when necessary from Cerro Negro, a
23 dark countryside environment at about 60 km north from Sevilla. Thus, we are
24 performing from Sevilla a continuous spectroscopic campaign since that year.
25 Nowadays, these spectral video cameras work continuously from 8 SPMN stations.
26 Favourable weather conditions in Spain play a key role in the successful development of
27 this spectroscopic campaign. In this context, we present here the analysis of four bolides
28 with a minimum brightness equivalent to an absolute magnitude of -10. These were
29 recorded over the Iberian Peninsula in the framework of our continuous fireball
30 monitoring and meteor spectroscopy campaigns performed between 2010 and 2012.

51 **2 INSTRUMENTATION AND DATA REDUCTION TECHNIQUES**

52 High-sensitivity monochrome CCD video cameras (models 902H2 and 902H Ultimate
53 from Watec Corporation, Japan) were employed to image the fireballs discussed here.
54 Thus, the bolides were recorded by an array of these video devices operating at the
55 meteor observing stations listed in Table 1. Some of these stations work in an
56
57
58
59
60

1
2
3 autonomous way by means of software developed by us (Madiedo & Trigo-Rodríguez
4 2010; Madiedo et al. 2010) and the cameras are arranged in such a way that the
5 common atmospheric volume monitored by neighbouring stations is maximized. These
6 devices generate interlaced imagery according to the PAL video standard. Thus, they
7 generate video files at a rate of 25 frames per second and with a resolution of 720x576
8 pixels. Aspherical fast lenses with focal lengths ranging from 6 to 20 mm and focal
9 ratios between 1.4 and 0.8 were used for the imaging objective lens. In this way,
10 different areas of the sky were covered by every camera and point-like star images were
11 obtained across the entire field of view. With this configuration we can image meteors
12 with an apparent magnitude of about 3 ± 1 . A more detailed description of the operation
13 of these systems is given in (Madiedo & Trigo-Rodríguez 2008, 2010).
14
15
16
17
18
19
20
21
22

23 For meteor spectroscopy we employ holographic diffraction gratings (500 or 1000
24 lines/mm, depending on the device) attached to the objective lens of some of the above-
25 mentioned cameras to image the emission spectra resulting from the ablation of
26 meteoroids in the atmosphere. We do not employ additional image intensifying devices.
27 We can image spectra for meteor events with brightness higher than mag. -3/-4.
28
29
30
31
32

33 With respect to data reduction, once that meteor trails simultaneously recorded from at
34 least two different meteor stations are identified, we first deinterlaced the video images
35 provided by our cameras. Thus, even and odd fields were separated for each video
36 frame, and a new video file containing these was generated. Since this operation implies
37 duplicating the total number of frames, the frame rate in the resulting video is 50 fps.
38 Then, an astrometric measurement is done by hand in order to obtain the plate (x, y)
39 coordinates of the meteor along its apparent path from each station. The astrometric
40 measurements are then introduced in our AMALTHEA software (Trigo-Rodríguez et al.
41 2009a; Madiedo et al. 2011a), which transforms plate coordinates into equatorial
42 coordinates by using the position of reference stars appearing in the images. This
43 package employs the method of the intersection of planes to determine the position of
44 the apparent radiant and also to reconstruct the trajectory in the atmosphere of meteors
45 recorded from at least two different observing stations (Ceplecha 1987). In this way, the
46 beginning and terminal heights of the meteor are inferred. From the sequential
47 measurements of the video frames and the trajectory length, the velocity of the meteor
48 along its path is obtained. The preatmospheric velocity V_{∞} is found from the velocity
49
50
51
52
53
54
55
56
57
58
59
60

1
2
3 measured in the earliest parts of the meteor trajectory. Once these data are known, the
4 software computes the orbital parameters of the corresponding meteoroid by following
5 the procedure described in Ceplecha (1987).
6
7

8 9 **3 OBSERVATIONS: atmospheric trajectory, radiant and orbit**

10 The fireballs analyzed here are listed in Table 2. Their SPMN code, which was assigned
11 after the recording date, is included for identification. The times of fireball passage are
12 known with a precision of 0.1 seconds. Besides, the bolides were named according to
13 the geographical location nearest to the projection on the ground of their atmospheric
14 trajectory. The beginning (H_b), ending (H_e) and maximum brightness (H_{max}) heights are
15 also indicated. As can be noticed, their absolute magnitude (M) ranges from -10.0 ± 0.5
16 to -11.0 ± 0.5 . These magnitudes were calculated by direct comparison of the brightness
17 level of the pixels near the maximum luminosity of the meteor trail and those of nearby
18 stars. Each bolide was simultaneously recorded from, at least, two of the observing
19 stations listed in Table 1. The radiant and orbital data obtained from the analysis of
20 these events are summarized in Table 3. These bolides are described in more detail
21 below.
22
23
24
25
26
27
28
29
30
31

32 **3.1 The "La Carlota" fireball (SPMN180910)**

33 This sporadic fireball, which reached the end of its luminous phase next to the zenith of
34 the city after which it was named, was simultaneously imaged from stations #1 and #9
35 on September 18, 2010 (Figure 1). The event, with an estimated absolute magnitude of -
36 11.0 ± 0.5 , began at 20h04m27.0 \pm 0.1s UTC at a height of 85.8 \pm 0.5 km above the ground
37 level and lasted about 4.5 seconds. The preatmospheric velocity of the meteoroid was
38 21.7 \pm 0.3 km s⁻¹, with the apparent radiant located at $\alpha=300.8 \pm 0.7^\circ$, $\delta=45.9 \pm 0.3^\circ$. The
39 bolide penetrated the atmosphere till a height of 25.6 \pm 0.5 km. The projection on the
40 ecliptic plane of the heliocentric orbit of the meteoroid is shown in Figure 1d. The
41 calculated orbital period yields $P=5.9 \pm 0.5$ yr, and the value obtained for the Tisserand
42 parameter with respect to Jupiter is $T_J=2.5 \pm 0.1$. This reveals that the particle was
43 following a Jupiter Family Comet (JFC) orbit (orbital period $P < 20$ yr and Tisserand
44 parameter in the range $2 < T_J < 3$) before impacting the Earth.
45
46
47
48
49
50
51
52
53
54
55

56 **3.2 The "Doñana" fireball (SPMN250112)**

57
58
59
60

1
2
3 A mag. -10.1 ± 0.5 slow-moving fireball was simultaneously recorded from stations #1
4 and #5 (Sevilla and El Arenosillo) on January 25, 2012, at $20\text{h}20\text{m}07.3 \pm 0.1\text{s}$ UTC
5 (Figure 2). The apparent trajectory of this sporadic bolide, which lasted about 6
6 seconds, is shown in Figure 4c. The parent meteoroid struck the atmosphere with an
7 initial velocity $V_{\infty} = 14.7 \pm 0.3 \text{ km s}^{-1}$ and a zenith angle of 38.2° , with an apparent radiant
8 located at $\alpha = 42.3 \pm 0.3^{\circ}$, $\delta = 3.8 \pm 0.3^{\circ}$. The luminous phase began at $78.4 \pm 0.5 \text{ km}$ above
9 the ground level and ended at $26.4 \pm 0.5 \text{ km}$. This deep-penetrating fireball received the
10 name "Doñana", as its atmospheric path was located over this natural park in the south
11 of Spain. Once this trajectory was obtained, the orbital parameters of the meteoroid
12 were calculated (Table 3). The projection of this orbit on the ecliptic plane is plotted in
13 Figure 2d. The Tisserand parameter with respect to Jupiter ($T_J = 2.4 \pm 0.1$) and the orbital
14 period ($P = 8.3 \pm 1.8 \text{ yr}$) show that this sporadic event was also produced by a meteoroid
15 in a JFC orbit.
16
17
18
19
20
21
22
23
24
25
26

27 **3.3 The "Torrecera" fireball (SPMN150812)**

28 This bolide, which lasted about 2 seconds, was recorded from stations #1 and #5 on
29 August 15, 2012, at $23\text{h}44\text{m}39.2 \pm 0.1\text{s}$ UTC (Figure 3). According to the photometric
30 analysis of the images, the event reached an absolute magnitude of about -10.2 ± 0.5 . As
31 can be seen in Figures 4a and 4b, the fireball experienced a very bright fulguration at
32 the end of its luminous path as a consequence of the violent disruption of the parent
33 meteoroid. According to our analysis, the fireball began at a height of $104.5 \pm 0.5 \text{ km}$ and
34 ended at $80.0 \pm 0.5 \text{ km}$ above the ground level. The meteoroid struck the atmosphere
35 with an initial velocity $V_{\infty} = 27.1 \pm 0.3 \text{ km s}^{-1}$ and the apparent radiant was located at
36 $\alpha = 295.4 \pm 0.3^{\circ}$, $\delta = 60.2 \pm 0.2^{\circ}$. The projection on the ecliptic plane of the orbit of the
37 meteoroid in the Solar System is shown in Figure 3d. These results confirm the
38 association of this event with the kappa-Cygnid meteoroid stream.
39
40
41
42
43
44
45
46
47
48

49 **3.4 The "Peñaflor" bolide (SPMN121212)**

50 This mag. -10.0 ± 0.5 Geminid fireball was simultaneously imaged from Sevilla, La Hita,
51 and El Arenosillo on December 12, 2012 at $3\text{h}47\text{m}19.7 \pm 0.1\text{s}$ UTC (Figure 4). It was, in
52 fact, the brightest Geminid recorded by our team in 2012. The analysis of its
53 atmospheric path shows that the meteoroid struck the atmosphere with an initial
54 velocity $V_{\infty} = 39.0 \pm 0.3 \text{ km s}^{-1}$ and a zenith angle of 13.4° . The fireball, with an apparent
55
56
57
58
59
60

radiant located at $\alpha=116.2\pm0.3^\circ$, $\delta=35.1\pm0.3^\circ$, began at 101.6 ± 0.5 km above the ground level and ended at a height of 39.9 ± 0.5 km. It lasted about 2.7 seconds. The heliocentric orbit of the meteoroid is shown in Figure 4d.

4 RESULTS AND DISCUSSION

4.1 Light curves and initial masses

The light curves (pixel intensity in arbitrary units vs. time) for the fireballs listed in Table 2 are shown in Figures 5 to 8. As can be noticed, all these events exhibit their maximum brightness during the second half of their trajectory, a behaviour which is typical of fireballs produced by compact meteoroids (Murray et al. 1999; Campbell et al. 2000). For dustball meteoroids, however, this takes place earlier (Hawkes & Jones 1975). In particular, the SPMN150812 "Torrecera" κ -Cygnid bolide (Figure 3) showed a very bright fulguration at the end of its atmospheric path as a consequence of the catastrophic disruption of the meteoroid.

The initial photometric mass m_p of the parent meteoroids have been calculated from these light curves as the total mass lost due to the ablation process between the beginning of the luminous phase and the terminal point of the atmospheric trajectory of the bolides:

$$m_p = 2 \int_{t_b}^{t_e} I_p / (\tau v^2) dt \quad (1)$$

where t_b and t_e are, respectively, the times corresponding to the beginning and the end of the luminous phase. I_p is the measured luminosity of the fireball, which is related to the absolute magnitude M by means of

$$M = -2.5 \log(I_p) \quad (2)$$

For the estimation of the luminous efficiency τ , which depends on velocity, we have employed the equations given by Ceplecha & McCrosky (1976). The calculated values of the initial photometric mass for each bolide are listed in Table 4. Both "La Carlota"

1
2
3 and "Doñana" sporadic bolides were produced by dm-sized meteoroids with masses of
4 about 1.9 and 5.7 kg, respectively. The parent meteoroids of the "Fuencaliente" κ-
5 Cygnid and the "Peñaflor" Geminid fireballs were, however, smaller. Their mass was
6 around one tenth of the mass of the "Doñana" sporadic meteoroid (about 0.18 and 0.12
7 kg, respectively), despite their maximum luminosity was similar.
8
9
10

11 12 13 **4.2 Tensile strength**

14 As can be noticed in the composite images shown in Figures 1 to 4 and also in the
15 above discussed light curves plotted in Figures 5 to 8, the fireballs exhibited at least one
16 very bright flare along their atmospheric path. These events are typically produced by
17 the fragmentation of the meteoroids when these particles penetrate denser atmospheric
18 regions. Thus, once the overloading pressure becomes larger than the particle strength,
19 the particle breaks apart. Quickly after that, a bright flare is produced as a consequence
20 of the fast ablation of tiny fragments delivered to the thermal wave in the fireball's bow
21 shock. The so-called tensile (aerodynamic) strength S at which these breakups take
22 place can be calculated by means of the following equation (Bronshten 1981):
23
24
25
26
27
28
29
30

$$31 \quad S = \rho_{\text{atm}} \cdot v^2 \quad (3)$$

32
33
34

35 where v is the velocity of the meteoroid at the disruption point and ρ_{atm} the atmospheric
36 density at the height where the fracture takes place. The density can be calculated, for
37 instance, by employing the US standard atmosphere model (U.S. Standard Atmosphere
38 1976). This aerodynamic strength S can be used as an estimation of the tensile strength
39 of the meteoroid (Trigo-Rodriguez & Llorca 2006, 2007). The values obtained for the
40 fireballs analyzed in this work are summarized in Table 5, together with the
41 corresponding heights and velocities.
42
43
44
45
46
47

48 As Figure 5 shows, the SPMN180910 "La Carlota" fireball experienced its main
49 fulguration at the instant $t_1=2.5$ s after the event started its luminous phase, followed by
50 a second fulguration at the instant $t_2=3.3$ s. The images reveal that the corresponding
51 fragmentations were not catastrophic, as the remaining material continued penetrating in
52 the atmosphere. These took place, respectively, at a height of 51.3 ± 0.5 and 38.1 ± 0.5 km
53 above the ground level. In this way, we infer that the meteoroid exhibited the first flare
54
55
56
57
58
59
60

1
2
3 under a dynamic pressure of $(3.2\pm 0.4)\cdot 10^6$ dyn cm⁻², while the second flare considered
4 here took place at $(1.4\pm 0.4)\cdot 10^7$ dyn cm⁻². The latter value is similar to the tensile
5 strength found for stony meteorites (Consolmagno and Britt 1998; Consolmagno et al.
6 2006, 2008; Macke et al. 2011). This supports the idea of high-strength meteoroids
7 moving in JFC orbits. Thus, although in general cometary meteoroids have low tensile
8 strengths ranging from $\sim 10^3$ to $\sim 10^5$ dyn cm⁻² (Trigo-Rodríguez & Llorca 2006, 2007),
9 fireballs produced by high-strength meteoroids moving in cometary orbits have also
10 been reported. Examples of fireballs produced by high-strength meteoroids moving in
11 cometary orbits are the Karlštejn fireball (Spurný & Borovička 1999a,b), for which a
12 mechanical strength of about $7\cdot 10^6$ dyn cm⁻² was obtained, and the deep-penetrating
13 Bejar bolide (Trigo-Rodríguez et al. 2009b), for which the calculated tensile strength
14 was $14\cdot 10^7$ dyn cm⁻². Besides, there are evidences that even Leonid meteoroids, whose
15 parent body is Comet 55P/Tempel–Tuttle, contain also much stronger ingredients with
16 measured tensile strengths of about $2\cdot 10^7$ dyn cm⁻² (Spurný et al. 2000, Borovička &
17 Jenniskens 2000). Thus, some authors have proposed that cometary nuclei may also
18 contain compact materials analogous to (or identical to) CI and CM carbonaceous
19 chondrites (Lodders & Osborne 1999).
20
21
22
23
24
25
26
27
28
29
30
31

32
33 A similar behaviour is found for the SPMN250112 "Doñana" sporadic fireball (Figure
34 6), but also for the SPMN121212 "Peñaflor" Geminid bolide (Figure 8), in the sense
35 that two main flares taking place at different heights can be distinguished. As can be
36 seen in Table 4, for the "Doñana" event these flares took place under a dynamic
37 pressure of $(3.6\pm 0.4)\cdot 10^6$ and $(5.6\pm 0.4)\cdot 10^6$ dyn cm⁻², respectively. So, this fireball was
38 also produced by a tough meteoroid following a JFC orbit. On the other hand, the
39 aerodynamic pressure obtained for the flares exhibited by the "Peñaflor" bolide
40 ($(2.0\pm 0.4)\cdot 10^5$ and $(5.1\pm 0.4)\cdot 10^5$ dyn cm⁻²) are close to the tensile strength values
41 previously obtained for other members of the Geminid meteoroid stream by Trigo-
42 Rodríguez & Llorca (2006, 2007). The SPMN150812 "Torrecera" κ -Cygnid bolide,
43 however, exhibited only one flare corresponding to the catastrophic disruption of the
44 meteoroid at the end of its luminous phase (Figure 7). This break-up took place at a
45 height of 80.0 ± 0.5 km. The calculation of the aerodynamic strength yields $(1.1\pm 0.4)\cdot 10^5$
46 dyn cm⁻². This value is of the same order of magnitude than those previously
47 determined for the other κ -Cygnids (Trigo-Rodríguez et al. 2009a).
48
49
50
51
52
53
54
55
56
57
58
59
60

4.3 Emission spectra

Our spectral cameras obtained the emission spectrum of the above discussed fireballs, except for the SPMN180910 ("La Carlota") event. These can be used to obtain an insight into the chemical nature of the parent meteoroids. We have employed our CHIMET software to process these spectra (Madiedo et al. 2011b). This application follows the analysis procedure described in Trigo-Rodríguez et al. (2003). Thus, the video frames containing the emission spectrum were dark-frame subtracted and flat-fielded. Then, the signal was calibrated in wavelengths by identifying typical lines appearing in meteor spectra (Ca, Fe, Mg and Na multiplets) and corrected by taking into account the efficiency of the recording instrument. The result can be seen in Figures 9 to 11. Multiplet numbers are given according to Moore (1945). For the "Peñaflor" and "Torrecera" bolides the emission spectrum is dominated by the lines of Mg I-2 (517.2 nm) and several Fe I multiplets: Fe I-41 (441.5 nm) and Fe I-15 (526.9 and 542.9 nm). In the ultraviolet, the intensity of H and K lines of ionized calcium are also strong, also blended with Fe I-4 due to the moderately low spectral resolution. The contribution from Na I-1 is also noticeable. The emission from atmospheric N₂ bands can also be noticed in the red region. The "Peñaflor" fireball, due to its higher velocity, exhibits a distinctive ionized Si II-2 line at 634.7 nm. On the other hand, the "Doñana" emission spectrum is characteristic of a low-velocity fireball mostly dominated by Fe I and Na I-1 lines and with a weaker Mg I-2 line than the "Torrecera" and "Peñaflor" events (Trigo-Rodríguez, 2002, Trigo-Rodríguez et al., 2003; 2004).

Once the main emission lines were identified, the relative abundances of the main rock-forming elements in the meteoroids were calculated. Thus, a software application was used to reconstruct a synthetic spectrum by adjusting the temperature (T) in the meteor plasma, the column density of atoms (N), the damping constant (D) and the surface area (P) from the observed brightness of lines as explained in Trigo-Rodríguez et al. (2003). First, as Fe I emission lines are well distributed all over the spectrum, they were used to set the parameters capable to fit the observed spectrum with the synthetic one (Trigo-Rodríguez et al. 2003, 2004). The modelled spectrum of the meteor column is then compared line by line with the observed one to fit all its peculiarities. Thus, once the parameters T, D, P and N are fixed, the relative abundances of the main rocky elements relative to Fe are found by performing an iterative process until an optimal fit is

1
2
3 achieved. To obtain the elemental abundances relative to Si, we have considered
4 Fe/Si=1.16 (Anders and Grevesse 1989). This was not needed for the Peñafior bolide
5 due to the possibility to obtain directly the Si abundance in the meteor column. The
6 results are summarized in Table 6, where these relative abundances are compared with
7 those found for other undifferentiated bodies in the Solar System, such as comet
8 1P/Halley and the CI and CM groups of carbonaceous chondrites (Jessberger et al.
9 1988; Rietmeijer & Nuth 2000; Rietmeijer 2002; Trigo-Rodríguez et al. 2003). Overall,
10 the computed abundances suggest that the main rock-forming elements were available
11 in proportions close to those found in chondrites with the classic exception of Ca, whose
12 abundance in the meteor column is much lower as a consequence of being usually
13 forming part of refractory minerals that experience incomplete vaporization (Trigo-
14 Rodríguez et al. 2003).

23 **4.4 Terminal mass and meteorite survival**

24 Two of the events discussed here ("La Carlota" and "Doñana") penetrated deep enough
25 in the atmosphere to take into consideration the likely survival of a fraction of the mass
26 in the parent meteoroid. The meteoroid mass surviving the ablation process, m_E , can be
27 obtained from the following relationship (Ceplecha et al. 1983):

$$28 \quad m_E = \left(\frac{1.2\rho_E V_E^2}{(dv/dt)_E \rho_m^{2/3}} \right) \quad (4)$$

29 with v_E and $(dv/dt)_E$ being, respectively, the velocity and deceleration at the terminal
30 point of the luminous trajectory. ρ_m is the meteoroid density and ρ_E the air density at the
31 terminal height. This equation assumes that the surviving mass is spherical in shape.

32
33
34 In fact, the low altitude of the terminal point (25.6 ± 0.5 km) of the SPMN180910 "La
35 Carlota" bolide suggests that this sporadic fireball was a potential meteorite-dropping
36 event. At the end of its luminous phase, the velocity of the bolide was of about 6.7 km s^{-1}
37 and the calculation of the terminal mass of the meteoroid yields 40 ± 30 g. Despite this
38 mass is small, the landing point of the meteorite was estimated with our AMALTHEA
39 software, which models the dark flight of the meteoroid by following the method
40 described in (Ceplecha 1987). Atmospheric data provided by AEMET (the Spanish
41
42
43
44
45
46
47
48
49
50
51
52
53
54
55
56
57
58
59
60

1
2
3 meteorological agency) were used to take into account wind effects. The particle was
4 assumed to be spherical. According to this analysis, the likely landing point would be
5 located around the geographical coordinates 37.6769 ° N, 4.9162 ° W. This corresponds
6 to a cereal growing area at about 1.5 km from the village after which the fireball was
7 named. Yet, no meteorites were found.
8
9
10

11
12 On the other hand, the luminous phase of the SPMN250112 "Doñana" fireball ended at
13 26.4±0.5 km above the ground level. According to the calculated atmospheric
14 trajectory, at that point its velocity was of around 3.1 km s⁻¹. The terminal mass
15 obtained from Eq. (4), however, is of the order of 0.1 grams. So, we concluded that the
16 survival of meteorites was not very likely in this case.
17
18
19
20
21

22 **4.5. Implications for Jupiter family cometary structure and their delivery of** 23 **meteorites to Earth.** 24 25 26

27 The inferred physical behaviour, tensile strength and bulk chemistry of the two bolides
28 dynamically linked with JFCs (SPMN180910 and SPMN250112) suggest that some
29 materials released from this cometary family might be similar to (or identical to)
30 carbonaceous chondrites. Our results are also suggesting that this cometary family is a
31 potential meteorite-dropping source as previously noted (di Martino and Cellino 2004,
32 Gounelle et al. 2006). It is thought that the JFC are probably fragments of Kuiper Belt
33 Objects (Morbidelli 2008), and this is also suggested from its size distribution
34 (Snodgrass et al. 2011). The Kuiper Belt contains a reservoir of ice-rich bodies that has
35 preserved dynamical clues about early Solar System processes that have set up its
36 current structure (Morbidelli 2008, Jewitt 2008). The current Nice model of planetary
37 evolution has demonstrated to be capable of reproducing many features of our planetary
38 system (Gomes et al. 2005). In general it is thought that every comet experienced
39 different evolutionary histories, and this particular source of comets could be directly
40 associated with bodies scattered from the outer main belt about 3.9 Gyr ago (Morbidelli
41 et al. 2005, 2010). The inwards migration of Jupiter and Saturn produced a massive
42 scattering of bodies that could be injected in different cometary regions like the Kuiper
43 Belt. Then, we think that this evolutionary model might predict naturally the presence of
44 high-strength chondritic bodies in different populations, like e.g. the JFC region. On the
45 other hand, it is also true that bodies in such populations could have been subjected to
46
47
48
49
50
51
52
53
54
55
56
57
58
59
60

1
2
3 significant collisional histories. So their surfaces could be heavily brecciated, and their
4 interiors could contain compressed materials with higher strengths than usually
5 expected for comet-forming materials (Trigo-Rodríguez & Blum 2009). And again the
6 presence of high-strength materials from collisionally evolved comets fits well the
7 recently revisited scenario on the higher collisional rates suffered by cometary families
8 (Bottke et al. 2005, 2007, 2012).
9
10

11
12
13
14 Additionally, it has been recently found that the amount of shock experienced by
15 carbonaceous chondrites has direct effect on the bulk density of these materials (Macke
16 et al. 2011). It is also plausible that these materials trace the remains of disrupted
17 comets as was previously envisioned in a scenario proposed thanks to the observation of
18 a superbolide produced by a 1 m sized meteoroid dynamically associated with the
19 disappeared comet C/1919 Q2 Metcalf (Trigo-Rodríguez et al. 2009b). It is remarkable
20 that, due to the intrinsically high relative velocity of JFCs colliding with other bodies,
21 many of these collisions could be catastrophic, producing fragments like the ones
22 presented in this paper. From an astrobiological point of view it is remarkable that the
23 discovery of ocean-like water in 103P/Hartley 2 (Hartough et al. 2011) opens the
24 possibility that JFC meteoroids could have been an important source of water and
25 organics to Earth. This source is not only associated with sporadic events as those
26 presented here, since there are several important active meteoroid streams associated
27 with JFCs (Williams 2009). In fact, dynamically these streams are driven by the
28 gravitational perturbation of Jupiter. Consequently, we think that there is growing
29 evidence that JFCs can be formed, at least partially, by high-strength materials of
30 chondritic nature. We envision that those reaching the top atmosphere at grazing angles
31 and with moderate velocities (in other words, with the optimal geometrical conditions)
32 could be a source of meteorites, but also of ablation-generated volatiles to Earth's
33 atmosphere (Trigo-Rodríguez 2013).
34
35
36
37
38
39
40
41
42
43
44
45
46
47
48

49 **5 CONCLUSIONS**

50 We have described and analyzed four bright fireballs observed over Spain from 2010 to
51 2012. Our main conclusions are:
52
53
54

- 55 1) Except for the SPMN150812 "Torrecera" κ -Cygndid fireball, which ended its
56 luminous phase at an altitude of around 80 km above the ground level, the
57
58
59
60

1
2
3 rest of the events analyzed here were deep-penetrating bolides. In particular,
4 the terminal points of the SPMN180910 "La Carlota" and SPMN 250112
5 "Doñana" sporadic fireballs were located at a height of about 25.6 and 26.4
6 km, respectively.
7
8

- 9
10
11 2) The meteoroids that produced the sporadic "Doñana" and "La Carlota"
12 fireballs exhibited a relatively high strength. This is particularly true for the
13 parent meteoroid of the SPMN180910 "La Carlota" event, which exhibited
14 values close to those found for stony meteorites. The values obtained for the
15 κ -Cygnid and the Geminid events are very close to those previously reported
16 in the literature for other members of these meteoroid streams.
17
18 3) The calculation of the orbital elements show that, except for the "Peñaflor"
19 Geminid, the parent meteoroid of these events followed Jupiter-Family
20 Comet (JFC) orbits before impacting the Earth. So, our results support the
21 idea of high-strength meteoroids moving in JFC orbits.
22
23 4) The analysis of the atmospheric trajectory shows that the SPMN180910 "La
24 Carlota" fireball was a potential meteorite-dropper. However, the calculated
25 mass of the surviving material is below 100 grams.
26
27 5) The analysis of the intensity of the emission lines of the three fireballs with
28 available spectra suggests that the bolides "Peñaflor", "Torrecera" and
29 "Doñana" were produced by meteoroids of chondritic nature.
30
31 6) From an astrobiological point of view, the continuous delivery of high-
32 strength and large JFC meteoroids could place this family as an important
33 source of water and organics to Earth.
34
35
36
37
38
39
40
41
42
43
44
45
46
47
48
49
50

51 **ACKNOWLEDGEMENTS**

52 We acknowledge support from the Spanish Ministry of Science and Innovation (project
53 AYA2011-26522) and Junta de Andalucía (project P09-FQM-4555). We also thank the
54 AstroHita Foundation for its continuous support in the operation of the meteor
55 observing station located at La Hita Astronomical Observatory.
56
57
58
59
60

REFERENCES

Borovička J. and Jenniskens P., 2000, *Earth Moon and Planets*, 82, 399.

Bottke W.F. et al., 2005, *Icarus*, 179, 63.

Bottke W.F. et al., 2007, *Icarus*, 190, 203.

Bottke W.F. et al., 2012, *Nature*, 485, 78.

Bronshten V.A., 1981, *Geophysics and Astrophysics Monographs*. Reidel, Dordrecht.

Campbell M.D. et al., 2000, *Meteorit. & Planet. Sci.*, 35, 1259.

Ceplecha Z., 1987, *Bull. Astron. Inst. Cz.*, 38, 222.

Ceplecha Z. and McCrosky R.E., 1976, *Journal of Geophysical Research*, 81, 6257.

Ceplecha Z., Novakova-Jezkova M., Porubcan V., Kirsten T., Kiko J., Bocek J., 1983, *Bull. Astron. Inst. Cz.*, 34, 195.

Consolmagno G. J. and Britt D. T., 1998, *Meteoritics & Planetary Science*, 33, 1231.

Consolmagno G. J., Macke R. J., Rochette P., Britt D. T., and Gattacceca J., 2006, *Meteoritics & Planetary Science*, 41, 331.

Consolmagno G. J., Britt D. T., and Macke R. J., 2008, *Chemie der Erde-Geochemistry*, 68, 1.

di Martino M., Cellino A., 2004, In: *Mitigation of Hazardous Comets and Asteroids*, M. Belton, T.H. Morgan, N. Samarasinha, and D.K. Yeomans (eds.), CUP, Cambridge, UK, p. 153.

1
2
3 **Gomes R. et al., 2005, Nature, 435, 466.**
4

5
6 **Gounelle M., Spurny P., Bland P.A., 2006, MAPS, 41, 135.**
7

8
9 **Hartough et al., 2011, Nature, 478, 218.**
10

11
12 Hawkes R.L. and Jones J., 1975, MNRAS, 173, 339.
13

14
15
16 **Jewitt D., 2008, In: Trans-Neptunian Objects and Comets, K. Altwegg, W. Benz**
17 **and N. Thomas (eds.), Saas-Fee Advanced Course 35, Springer-Verlag, Berlin, p. 1.**
18

19
20
21 Lodders K. and Osborne R., 1999, Space Sci. Rev., 90, 289.
22

23
24 Macke R.J., Consolmagno G.J., and Britt D.T. et al., 2011, Meteoritics & Planetary
25 Science, 46, 1842.
26

27
28
29 Madiedo J.M., Trigo-Rodríguez J.M., 2008, Earth Moon Planets, 102, 133.
30

31
32
33 Madiedo J.M., Trigo-Rodríguez J.M., Ortiz J.L., Morales N., 2010, Advances in
34 Astronomy, 2010, 1.
35

36
37
38 Madiedo J.M., Trigo-Rodríguez J.M., Lyttinen, E., 2011a, NASA/CP-2011-216469,
39 330.
40

41
42
43 Madiedo J.M., Toscano F.M., Trigo-Rodríguez J.M., 2011b, EPSC-DPS Joint Meeting
44 2011, Abstract #Vol. 6, EPSC-DPS2011-72.
45

46
47
48 Madiedo J.M., Trigo-Rodríguez, J.M., Konovalova N., Williams I.P., Castro-Tirado
49 A.J., Ortiz J.L., Cabrera J., 2013a, MNRAS, doi:10.1093/mnras/stt748.
50

51
52
53 Madiedo J.M., Trigo-Rodríguez, J.M., Williams I.P., Ortiz J.L., Cabrera J., 2013b,
54 MNRAS, doi:10.1093/mnras/stt342.
55
56
57
58
59
60

1
2
3 Madiedo J.M., Trigo-Rodríguez, Lyytinen E., Dergham J., Pujols P., Ortiz J.L., Cabrera
4 J., 2013c, MNRAS, doi:10.1093/mnras/stt288.
5
6

7
8 **Morbidelli A., Levison H. F., Tsiganis K., Gomes R., 2005, Nature, 435, 462.**
9

10
11 **Morbidelli A., 2008, In: Trans-Neptunian Objects and Comets, K. Altwegg, W.**
12 **Benz and N. Thomas (eds.), Saas-Fee Advanced Course 35, Springer-Verlag,**
13 **Berlin, p. 79.**
14
15

16
17
18 **Morbidelli A., Brassier R., Gomes R., Levison H. F., Tsiganis K., 2010, AJ, 140,**
19 **1391.**
20

21
22
23 Moore C.E., 1945, In: A Multiplet Table of Astrophysical Interest. Princeton University
24 Observatory, Princeton, NJ. Contribution No. 20.
25

26
27
28 Murray I.S., Hawkes R.L., Jenniskens P., 1999, Meteorit. & Planet. Sci., 34, 949.
29

30
31 **Snodgrass C. et al., 2011, MNRAS, 414, 458.**
32

33
34 Spurný P. and Borovička J., 1999a, in: W.J. Baggaley & V. Porubčan (eds.),
35 Meteoroids, 1998, Bratislava: Astron. Inst. Slovak Acad. Sci., p. 143.
36
37

38
39 Spurný P. and Borovička J., 1999b, in: J. Svoren et al. (eds.), Evolution and Source
40 Regions of Asteroids and Comets, Tatranská Lomnica: Astron. Inst. Slovak Acad. Sci.,
41 p. 163.
42
43

44
45
46 Spurný P., Betlem H., Jobse K., Kotten P., Van't Leven J., 2000, Meteorit. Planet. Sci.
47 35, 1109.
48

49
50
51 **Trigo-Rodríguez, 2013, In: The Early Evolution of the Atmospheres of Terrestrial**
52 **Planets, Astrophysics & Space Science Proceedings 35, Springer, NY, p. 9.**
53
54

55
56 **Trigo-Rodríguez J.M., Blum J., 2009, PSS, 57, 243.**
57
58
59
60

1
2
3
4
5
6
7
8
9
10
11
12
13
14
15
16
17
18
19
20
21
22
23
24
25
26
27
28
29
30
31
32
33
34
35
36
37
38
39
40
41
42
43
44
45
46
47
48
49
50
51
52
53
54
55
56
57
58
59
60

Trigo-Rodríguez J. M., Llorca J., 2006, MNRAS, 372, 655.

Trigo-Rodríguez J. M., Llorca J., 2007, MNRAS, 375, 415.

Trigo-Rodríguez, J.M. et al., 2007, MNRAS 382, 1933.

Trigo-Rodríguez J.M., Llorca J., Borovička J., Fabregat J., 2003, Meteorit. Planet. Sci., 38, 1283.

Trigo-Rodríguez J.M., Madiedo J.M., Williams I.P., Castro-Tirado A.J., 2009a, MNRAS, 392, 367.

Trigo-Rodríguez J.M. et al., 2009b, MNRAS, 394, 569.

U.S. Standard Atmosphere, 1976, NOAA-NASA-USAF, Washington.

Williams I.P., 2009, PSS, 57, 1228.

TABLES

Table 1. Geographical coordinates of the meteor observing stations involved in this work.

| Station # | Station name | Longitude (W) | Latitude (N) | Alt. (m) |
|-----------|------------------|---------------|--------------|----------|
| 1 | Sevilla | 5° 58' 50" | 37° 20' 46" | 28 |
| 2 | La Hita | 3° 11' 00" | 39° 34' 06" | 674 |
| 3 | Huelva | 6° 56' 11" | 37° 15' 10" | 25 |
| 4 | Sierra Nevada | 3° 23' 05" | 37° 03' 51" | 2896 |
| 5 | El Arenosillo | 6° 43' 58" | 37° 06' 16" | 40 |
| 7 | Molina de Segura | 1° 09' 50" | 38° 05' 54" | 94 |

Table 2. Absolute magnitude (M), trajectory and geocentric radiant data (J2000) for the fireballs analyzed in this work. The values of the beginning (H_b), ending (H_e) and maximum brightness (H_{max}) heights are indicated. V_∞ , V_g and V_h are the observed preatmospheric, geocentric and heliocentric velocity, respectively.

| SPMN Code and name | Date | Time (UTC) $\pm 0.1s$ | M | H_b (km) | H_{max} (km) | H_e (km) | α_g ($^\circ$) | δ_g ($^\circ$) | V_∞ ($km\ s^{-1}$) | V_g ($km\ s^{-1}$) | V_h ($km\ s^{-1}$) |
|------------------------|------------------|-----------------------|--------------------|--------------------|-------------------|-------------------|-------------------------|-------------------------|-----------------------------|------------------------|------------------------|
| 180910 "La Carlota" | Sep. 18, 2010 | 20h04m27.0s | -11.0 ± 0.5 | 85.8 ± 0.5 | 51.3 ± 0.5 | 25.6 ± 0.5 | 298.5 ± 0.7 | 46.4 ± 0.3 | 21.7 ± 0.3 | 18.7 ± 0.3 | 38.7 ± 0.3 |
| 250112 "Doñana" | Jan. 25, 2012 | 20h20m07.3s | -10.1 ± 0.5 | 78.4 ± 0.5 | 37.2 ± 0.5 | 26.4 ± 0.5 | 34.5 ± 0.3 | -3.8 ± 0.3 | 14.7 ± 0.3 | 9.9 ± 0.4 | 39.8 ± 0.4 |
| 150812 "Torrecera" | Aug. 15, 2012 | 23h44m39.2s | -10.2 ± 0.5 | 104.5 ± 0.5 | 80.0 ± 0.5 | 80.0 ± 0.5 | 291.3 ± 0.3 | 60.6 ± 0.3 | 27.1 ± 0.3 | 24.8 ± 0.3 | 37.6 ± 0.3 |
| 121212 "Peñaflor" | Dec. 12, 2012 | 3h47m19.7s | -10.0 ± 0.5 | 101.6 ± 0.5 | 65.3 ± 0.5 | 39.9 ± 0.5 | 114.8 ± 0.3 | 34.9 ± 0.3 | 39.0 ± 0.3 | 37.5 ± 0.3 | 34.9 ± 0.3 |

Table 3. Orbital elements (J2000) and Tisserand parameter with respect to Jupiter (T_J) for the bolides discussed in the text.

| SPMN Code and name | a (AU) | e | i (°) | Ω (°) | ω (°) | q (AU) | T_J |
|------------------------|-----------|-------------|----------|---------------------------|-----------------|---------------|---------|
| 180910 "La Carlota" | 3.4±0.2 | 0.71±0.02 | 26.4±0.3 | 175.6521±10 ⁻⁴ | 205.0±0.6 | 0.965±0.001 | 2.5±0.1 |
| 250112 "Doñana" | 4.1±0.6 | 0.76±0.04 | 4.0±0.1 | 125.0826±10 ⁻⁴ | 357.0±0.3 | 0.9839±0.0001 | 2.4±0.1 |
| 150812 "Torrecera" | 2.6±0.1 | 0.62±0.01 | 40.8±0.4 | 143.3539±10 ⁻⁴ | 199.8±0.3 | 0.9895±0.0007 | 2.8±0.1 |
| 121212 "Peñaflor" | 1.52±0.04 | 0.920±0.003 | 36.2±0.8 | 260.3488±10 ⁻⁴ | 326.0±0.5 | 0.120±0.003 | 3.7±0.1 |

Table 4. Photometric mass (m_p) and estimated diameter (D) of each meteoroid.

| SPMN Code and name | m_p (kg) | D (cm) ($d=2.4 \text{ g cm}^{-3}$) | D (cm) ($d=3.7 \text{ g cm}^{-3}$) |
|------------------------|------------|---|---|
| 180910 "La Carlota" | 1.9±0.2 | 11.4±0.3 | 9.9±0.3 |
| 250112 "Doñana" | 5.7±0.6 | 16.5±0.6 | 14.3±0.5 |
| 150812 "Torrecera" | 0.18±0.02 | 5.2±0.2 | 4.5±0.2 |
| 121212 "Peñaflor" | 0.12±0.01 | 4.5±0.1 | 3.9±0.1 |

Table 5. Aerodynamic pressure for flares and break-up processes discussed in the text.

| SPMN Code and name | Flare # | Height (km) | Velocity (km s^{-1}) | Aerodynamic pressure (dyn cm^{-2}) |
|------------------------|------------|----------------|------------------------------------|--|
| 180910 "La Carlota" | 1 | 51.3±0.5 | 19.6±0.3 | (3.2±0.4)·10 ⁶ |
| 250112 "Doñana" | 2 | 38.1±0.5 | 16.9±0.3 | (1.4±0.4)·10 ⁷ |
| 150812 "Torrecera" | 1 | 43.1±0.5 | 12.1±0.3 | (3.6±0.4)·10 ⁶ |
| 121212 "Peñaflor" | 2 | 37.2±0.5 | 9.8±0.3 | (5.6±0.4)·10 ⁶ |
| 150812 "Torrecera" | 1 | 80.0±0.5 | 26.1±0.3 | (1.1±0.4)·10 ⁵ |
| 121212 "Peñaflor" | 1 | 65.3±0.5 | 37.4±0.3 | (2.0±0.4)·10 ⁵ |
| 121212 "Peñaflor" | 2 | 57.1±0.5 | 35.1±0.3 | (5.1±0.4)·10 ⁵ |

Table 6. Relative abundances with respect to Si of the main rock-forming elements derived from the analysis of emission spectra.

| SPMN Code and name | T (K) ±100 | N (cm ⁻²) | Mg | Na | Fe | Ca | Mn (×10 ⁻⁴) |
|-----------------------|---------------|--------------------------|------|-------|-------|-------|----------------------------|
| 250112 "Doñana" | 4,200 | 1·10 ¹⁴ | 0,77 | 0,05 | - | 0,023 | - |
| 150812 "Torrecera" | 4,500 | 1·10 ¹⁵ | 0.80 | 0,05 | - | 0,028 | 25 |
| 121212 "Peñaflor" | 4,800 | 5·10 ¹⁵ | 1.03 | 0,04 | 0,82 | 0,026 | - |
| 1P/Halley | - | - | 0.54 | 0.054 | 0.280 | 0.034 | 30 |
| IDPs | - | - | 0.85 | 0.085 | 0.63 | 0.048 | 150 |
| CI chondrites | - | - | 1.06 | 0.060 | 0.90 | 0.071 | 90 |
| CM chondrites | - | - | 1.04 | 0.035 | 0.84 | 0.072 | 60 |

1
2
3
4
5
6
7
8
9
10
11
12
13
14
15
16
17
18
19
20
21
22
23
24
25
26
27
28
29
30
31
32
33
34
35
36
37
38
39
40
41
42
43
44
45
46
47
48
49
50
51
52
53
54
55
56
57
58
59
60

1
2
3
4
5
6
7
8
9
10
11
12
13
14
15
16
17
18
19
20
21
22
23
24
25
26
27
28
29
30
31
32
33
34
35
36
37
38
39
40
41
42
43
44
45
46
47
48
49
50
51
52
53
54
55
56
57
58
59
60

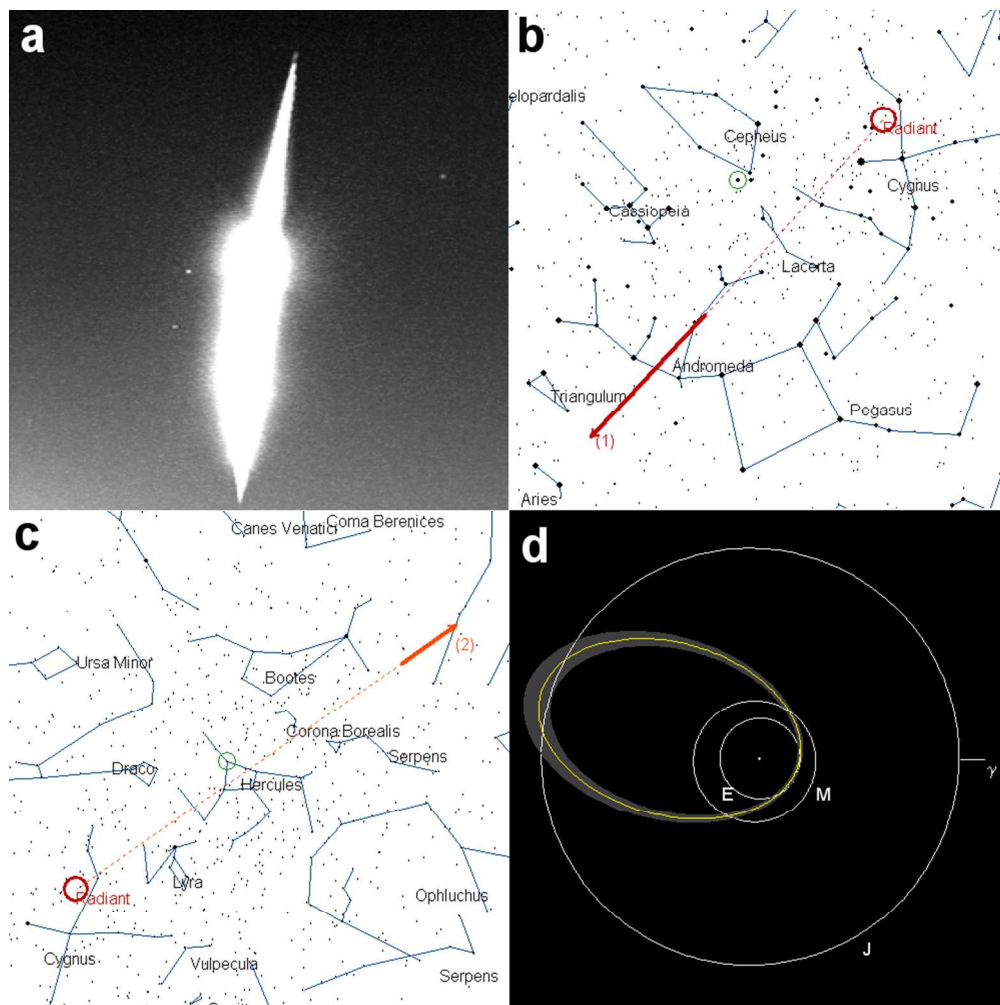


Figure 1. a) Composite image of the sporadic "La Carlota" fireball (code SPMN180910), imaged on Sep. 18, 2010 at 20h04m27.0±0.1s UTC from Sevilla. b) Apparent trajectory of the bolide as seen from Sevilla and c) La Murta meteor observing stations. d) Heliocentric orbit of the meteoroid projected on the ecliptic plane.

The gray area represents the uncertainty in the orbit by taking into account the uncertainty in the semimajor axis.

352x352mm (72 x 72 DPI)

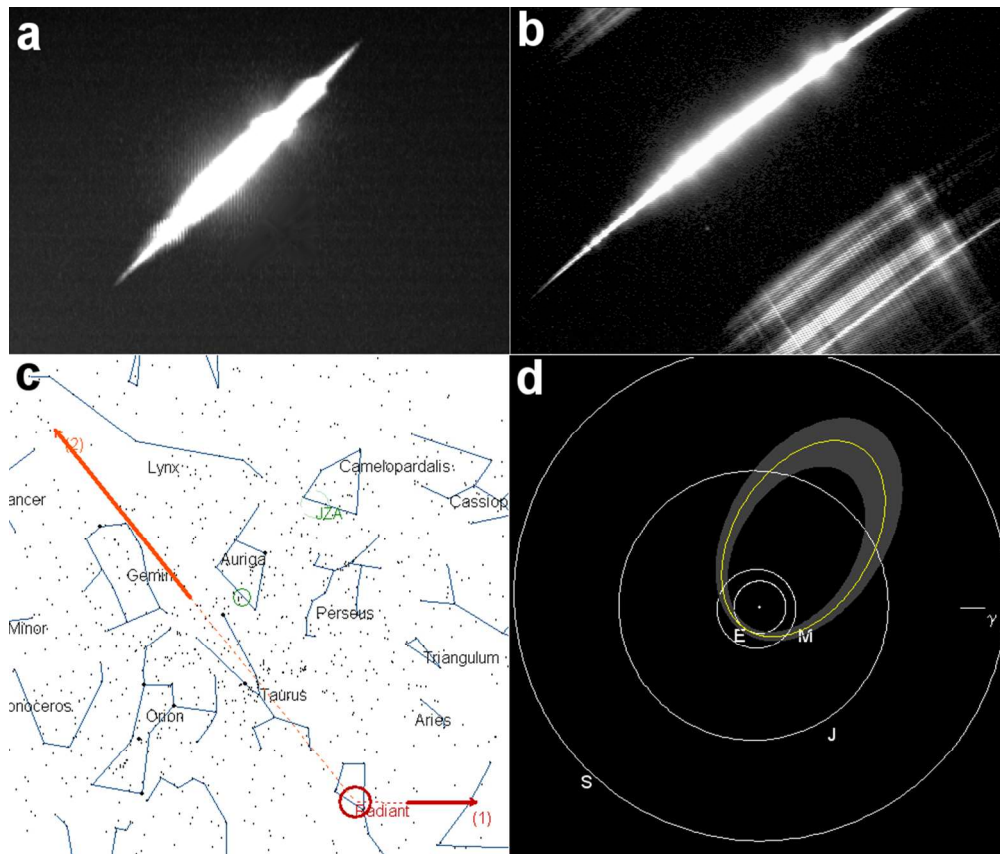


Figure 2. a) Composite image of the "Doñana" fireball (code SPMN250112), imaged on Jan. 25, 2012 at 20h20m07.3±0.1s UTC from a) Sevilla and b) El Arenosillo. c) Apparent trajectory of the bolide as seen from Sevilla (1) and El Arenosillo (2). d) Heliocentric orbit of the meteoroid projected on the ecliptic plane. The gray area represents the uncertainty in the orbit by taking into account the uncertainty in the semimajor axis.

352x299mm (72 x 72 DPI)

1
2
3
4
5
6
7
8
9
10
11
12
13
14
15
16
17
18
19
20
21
22
23
24
25
26
27
28
29
30
31
32
33
34
35
36
37
38
39
40
41
42
43
44
45
46
47
48
49
50
51
52
53
54
55
56
57
58
59
60

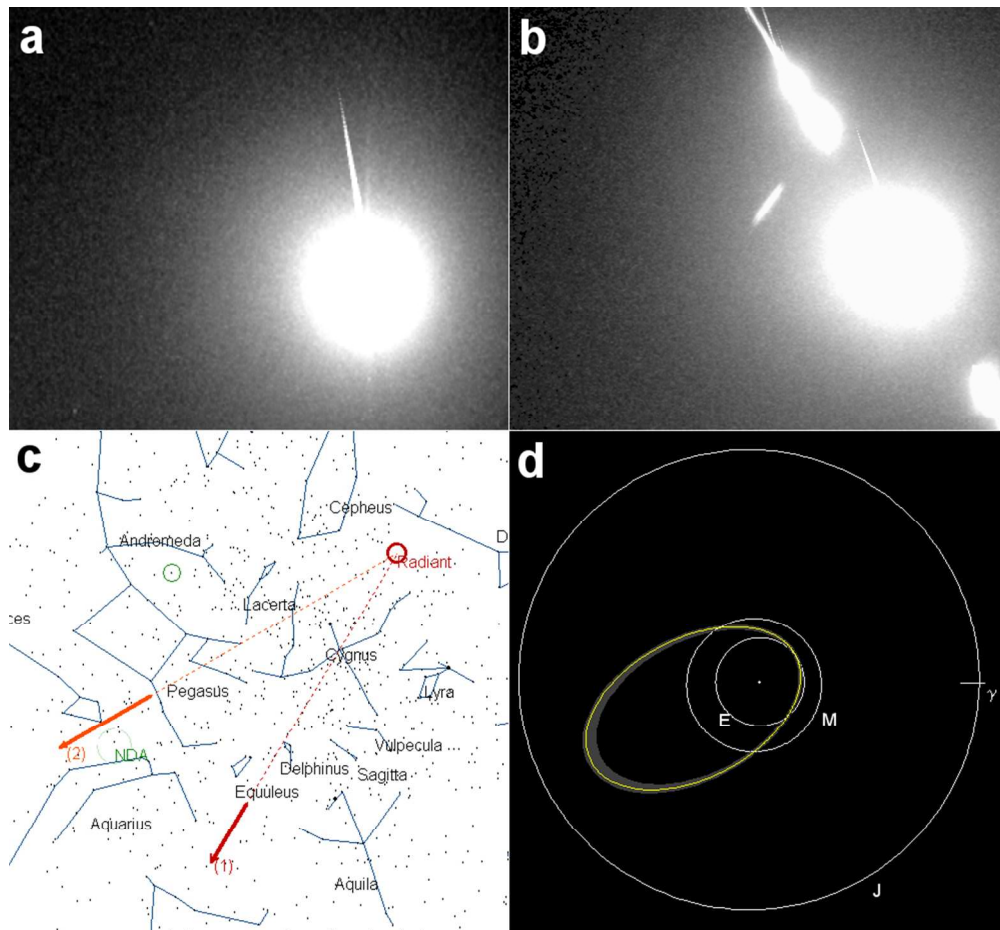


Figure 3. Composite image of the "Torrecera" κ -Cygnid fireball (code SPMN150812), imaged on Aug. 15, 2012 at 23h44m39.2 \pm 0.1s UTC from a) Sevilla and b) El Arenosillo. c) Apparent trajectory of the bolide as seen from Sevilla (1) and El Arenosillo (2). d) Heliocentric orbit of the meteoroid projected on the ecliptic plane. The gray area represents the uncertainty in the orbit by taking into account the uncertainty in the semimajor axis.

352x325mm (72 x 72 DPI)

1
2
3
4
5
6
7
8
9
10
11
12
13
14
15
16
17
18
19
20
21
22
23
24
25
26
27
28
29
30
31
32
33
34
35
36
37
38
39
40
41
42
43
44
45
46
47
48
49
50
51
52
53
54
55
56
57
58
59
60

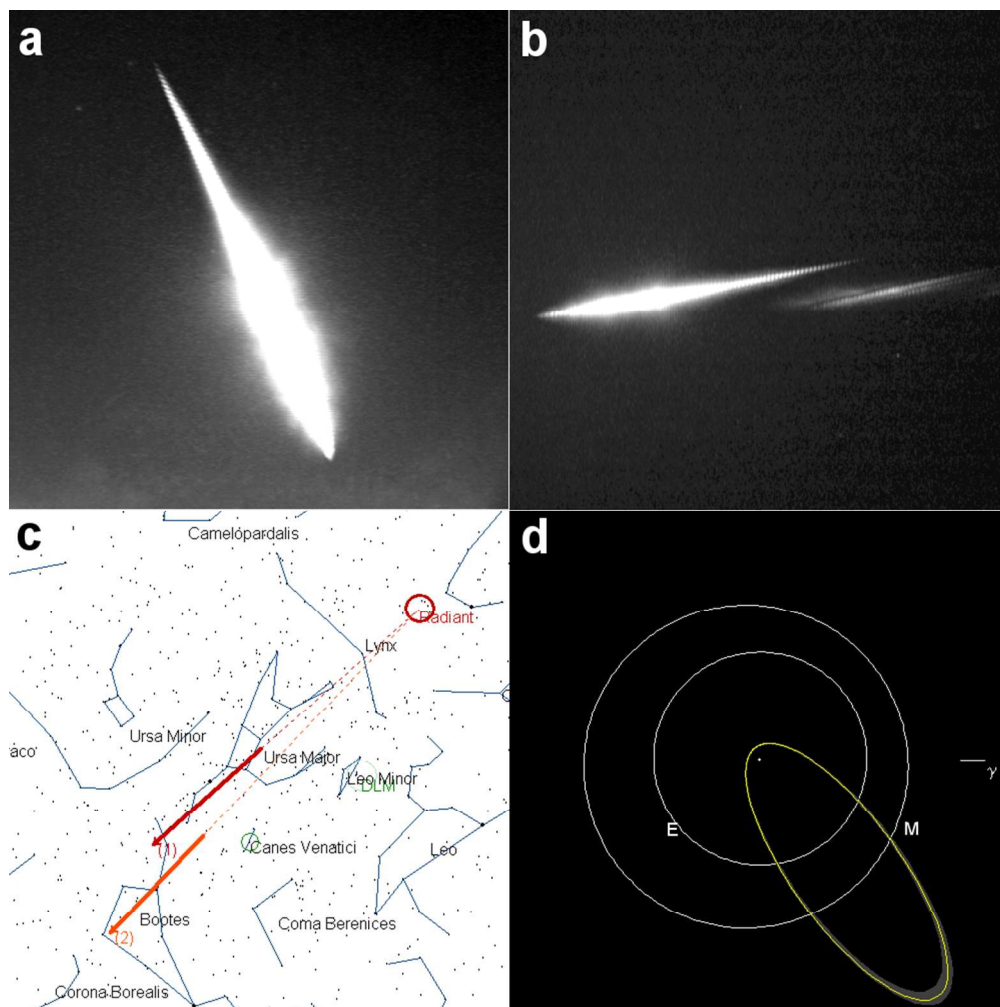


Figure 4. Composite image of the "Peñaflor" Geminid fireball (code SPMN121212), imaged on Dec. 12, 2012 at $3\text{h}47\text{m}19.7 \pm 0.1\text{s}$ UTC from a) Sevilla and b) El Arenosillo. c) Apparent trajectory of the bolide as seen from (1) Sevilla and (2) El Arenosillo. d) Heliocentric orbit of the meteoroid projected on the ecliptic plane.

The gray area represents the uncertainty in the orbit by taking into account the uncertainty in the semimajor axis.

352x352mm (72 x 72 DPI)

1
2
3
4
5
6
7
8
9
10
11
12
13
14
15
16
17
18
19
20
21
22
23
24
25
26
27
28
29
30
31
32
33
34
35
36
37
38
39
40
41
42
43
44
45
46
47
48
49
50
51
52
53
54
55
56
57
58
59
60

1
2
3
4
5
6
7
8
9
10
11
12
13
14
15
16
17
18
19
20
21
22
23
24
25
26
27
28
29
30
31
32
33
34
35
36
37
38
39
40
41
42
43
44
45
46
47
48
49
50
51
52
53
54
55
56
57
58
59
60

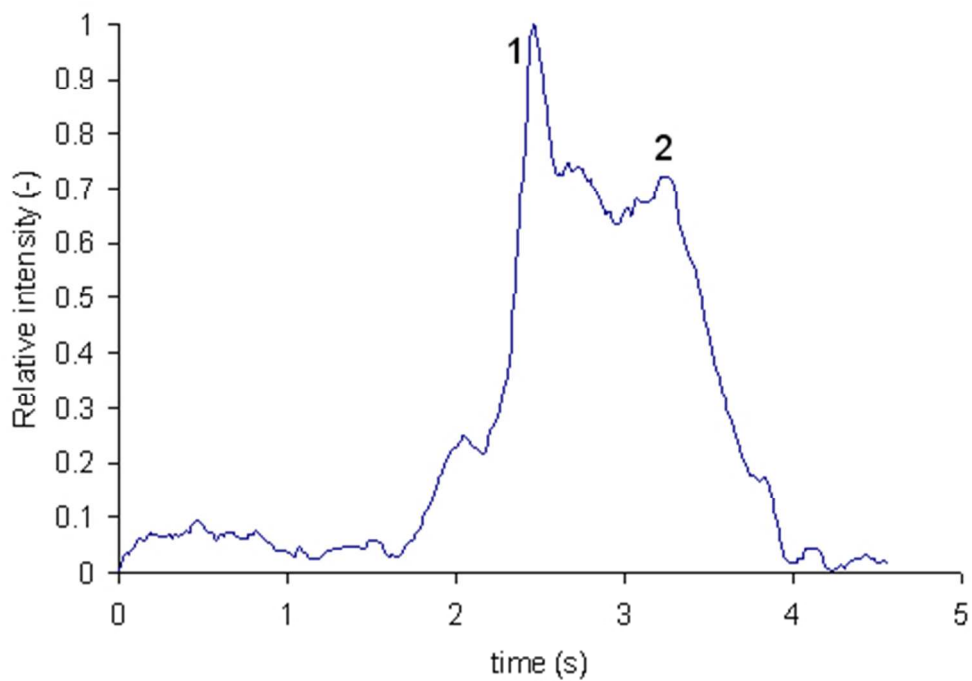


Figure 5. Light curve (relative pixel intensity vs. time) of the SPMN180910 "La Carlota" fireball.
178x127mm (72 x 72 DPI)

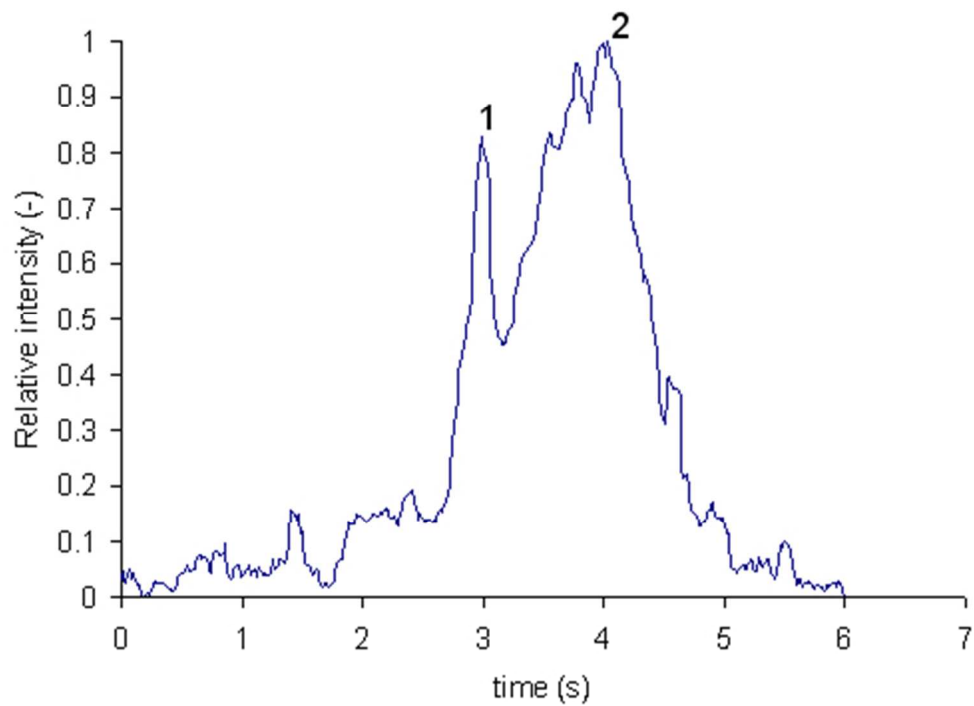


Figure 6. Light curve (relative pixel intensity vs. time) of the SPMN250112 "Doñana" fireball.
177x128mm (72 x 72 DPI)

1
2
3
4
5
6
7
8
9
10
11
12
13
14
15
16
17
18
19
20
21
22
23
24
25
26
27
28
29
30
31
32
33
34
35
36
37
38
39
40
41
42
43
44
45
46
47
48
49
50
51
52
53
54
55
56
57
58
59
60

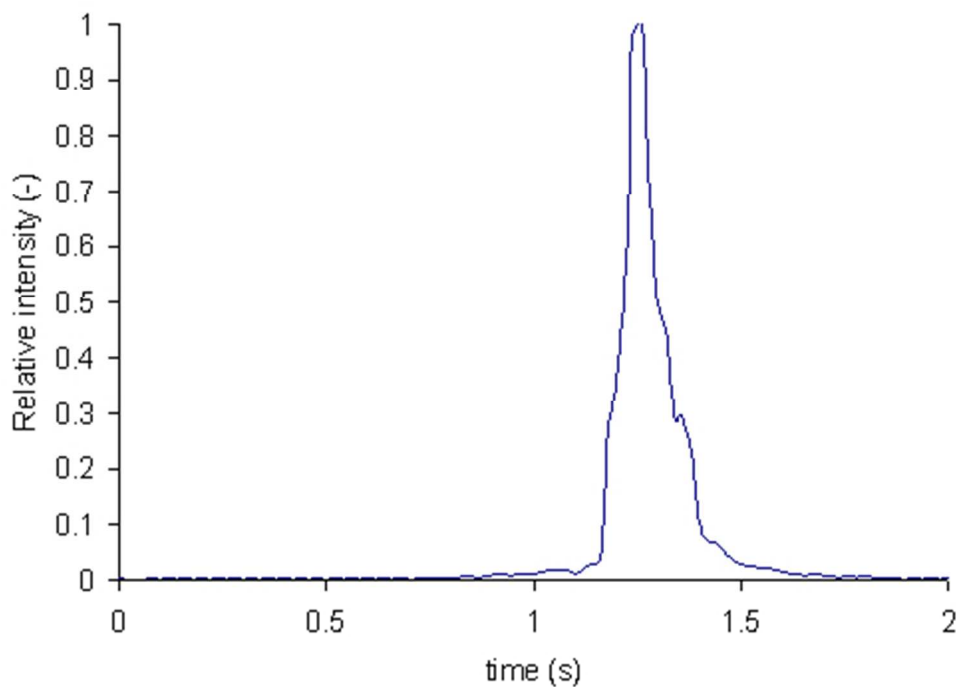


Figure 7. Light curve (relative pixel intensity vs. time) of the SPMN150812 "Torrecera" κ -Cygnid bolide.
177x128mm (72 x 72 DPI)

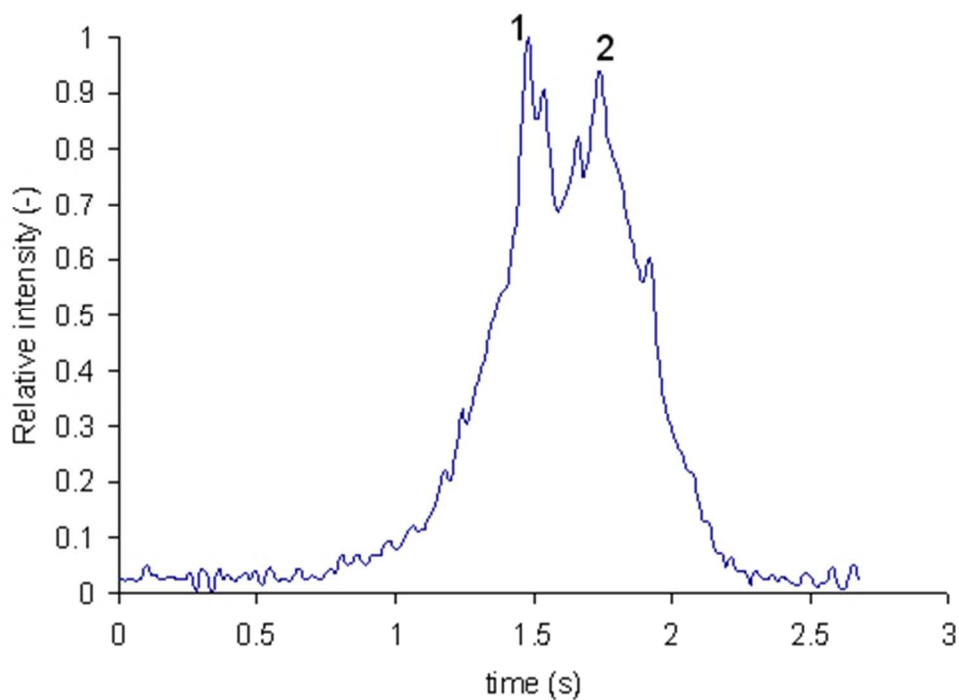


Figure 8. Light curve (relative brightness vs. time) of the SPMN121212 "Peñaflor" fireball. Main fulgurations for which the aerodynamic pressure was calculated are highlighted.
177x128mm (72 x 72 DPI)

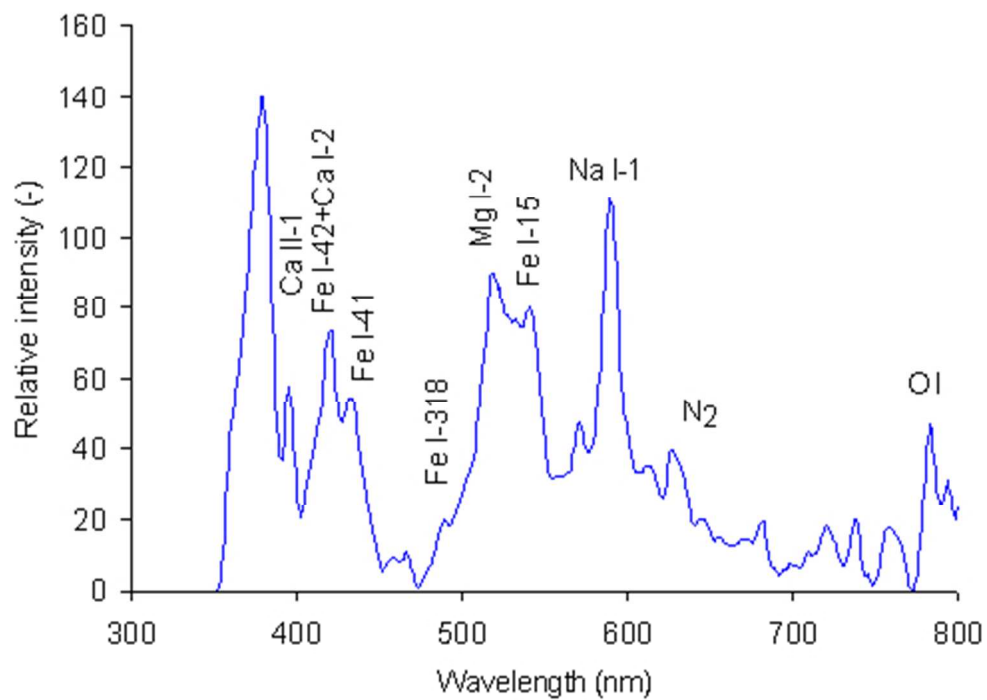


Figure 9. Calibrated emission spectrum recorded for the SPMN250112 "Doñana" fireball. Intensity is expressed in arbitrary units.
177x127mm (72 x 72 DPI)

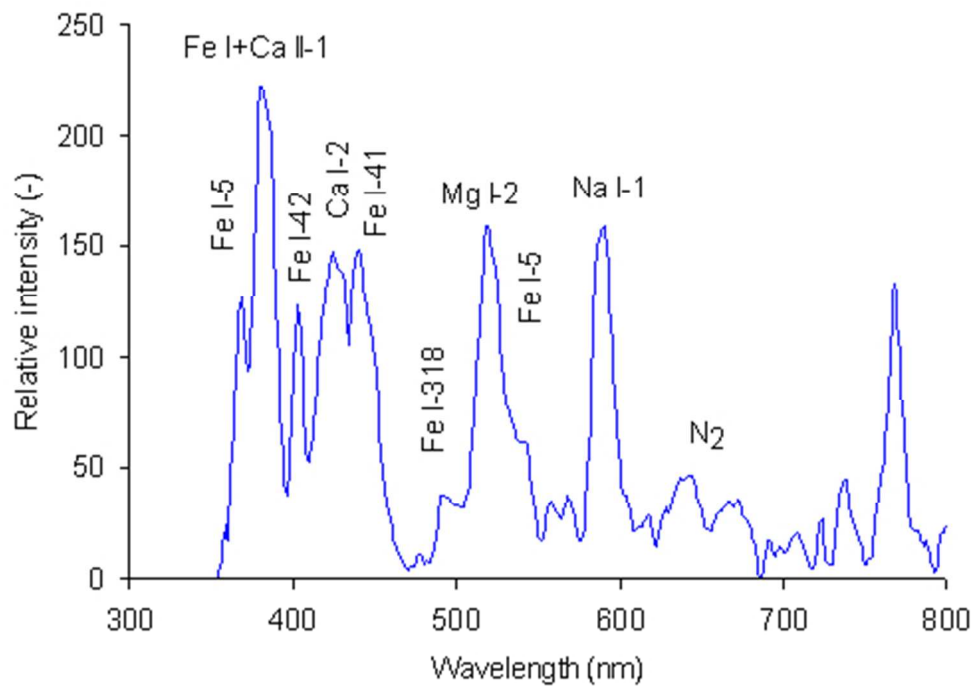


Figure 10. Calibrated emission spectrum recorded for the SPMN150812 "Torrecera" κ -Cygnid bolide.
Intensity is expressed in arbitrary units.
178x128mm (72 x 72 DPI)

1
2
3
4
5
6
7
8
9
10
11
12
13
14
15
16
17
18
19
20
21
22
23
24
25
26
27
28
29
30
31
32
33
34
35
36
37
38
39
40
41
42
43
44
45
46
47
48
49
50
51
52
53
54
55
56
57
58
59
60

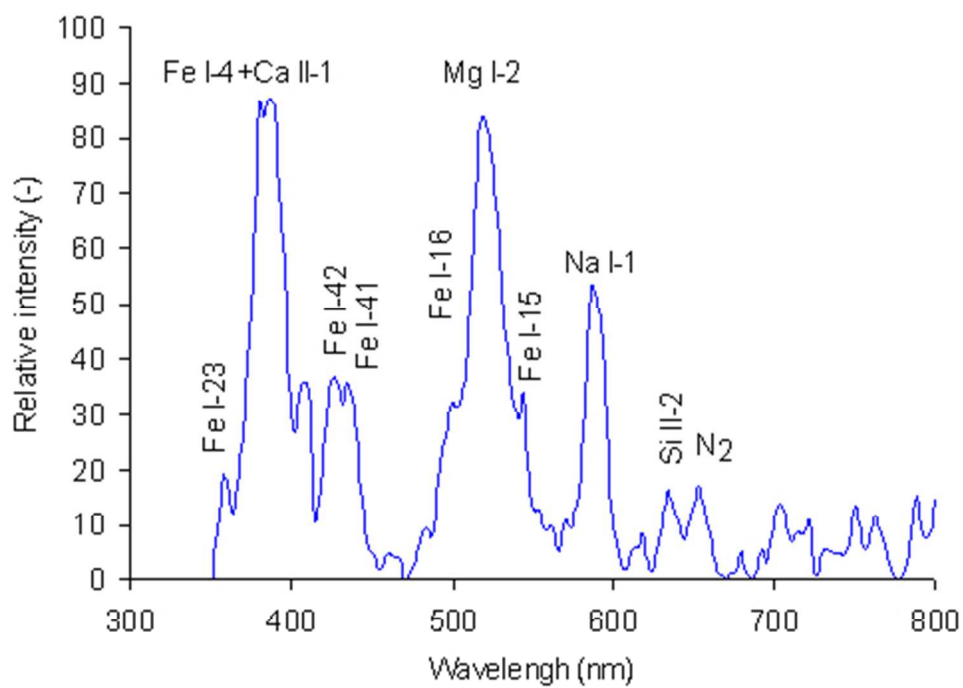


Figure 11. Calibrated emission spectrum recorded for the SPMN121212 "Peñaflor" Geminid bolide. Intensity is expressed in arbitrary units.
177x128mm (72 x 72 DPI)